Supporting Information

Core-shell CuO@NiCoMn-LDH supported by copper foam for high-performance supercapacitors

Lu Wang[a], Junhua You[a,*], Yao Zhao[a], Wanting Bao[a]

[a] School of Materials Science and Engineering, Shenyang University of Technology, Shenyang 110870, China

Corresponding authors: youjunhua168@163.com

Characterization

Samples were characterized by scanning electron microscopy (SEM, Zeiss Supra 55) and the surface chemical compositions were identified on a Thermo Escalab 250Xi X-ray photoelectron spectroscopy (XPS) device. X-ray diffraction (XRD) patterns were recorded on a D/Max-RB X-ray diffractometer. Raman spectroscopy (Horiba LabRAM confocal Raman spectrometer with an excitation laser of 632.8 nm). Transmission electron microscopy (TEM) measurements were characterized on an FEI Tecnai F30 electron microscope at an accelerating voltage of 300 kV.

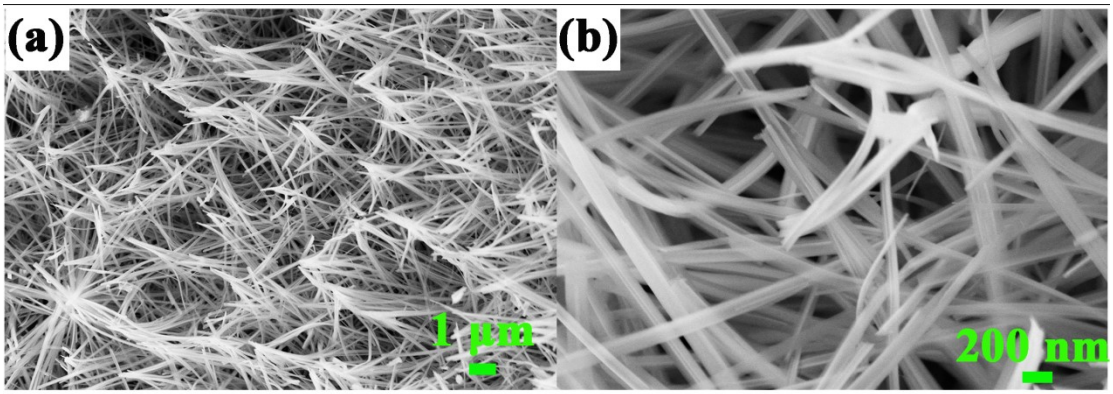

Fig. S1. SEM image of $Cu(OH)_2$ nanowires grown on CF.

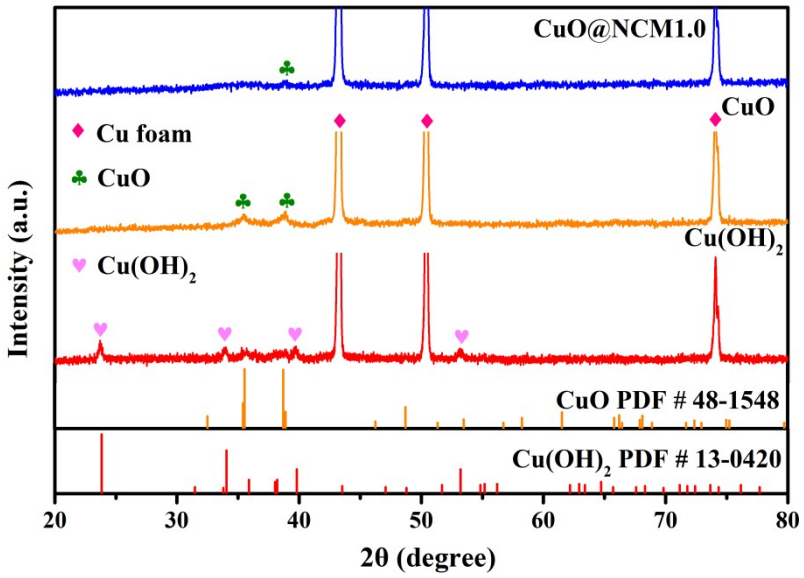

Fig. S2 XRD patterns of the as-prepared $Cu(OH)_2$, CuO and CuO@NCM1.0.

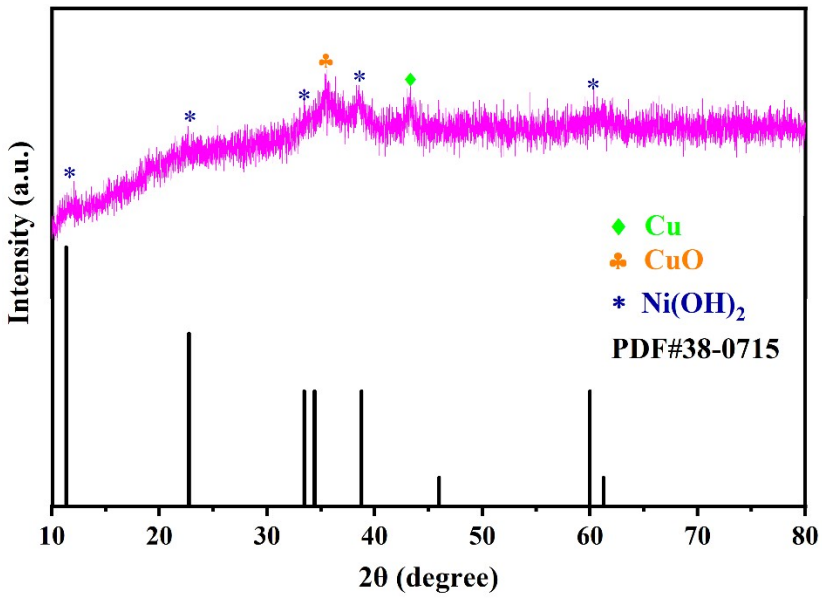

Fig. S3. The XRD pattern of CuO@NCM1.0 peeled off from the CF.

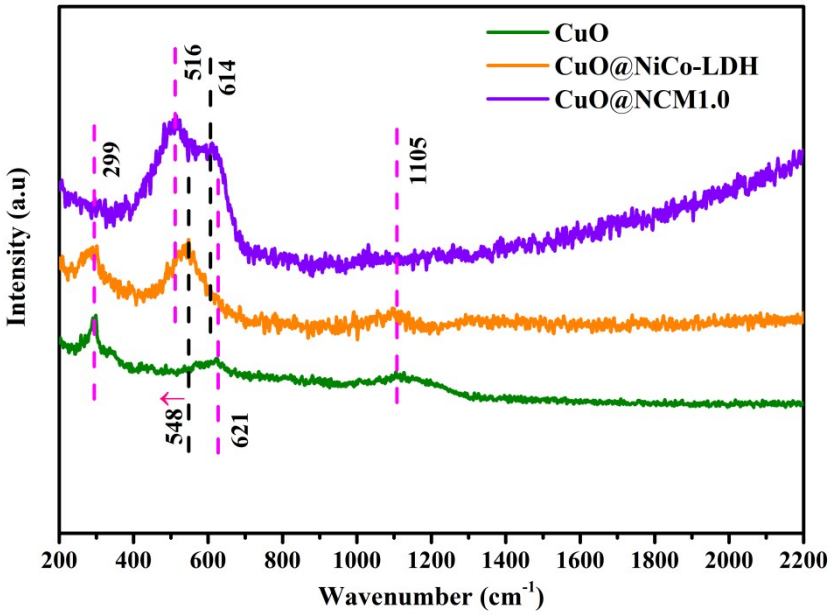

Fig. S4 Raman spectra of the CuO, CuO@NiCo-LDH, CuO@NCM1.0.

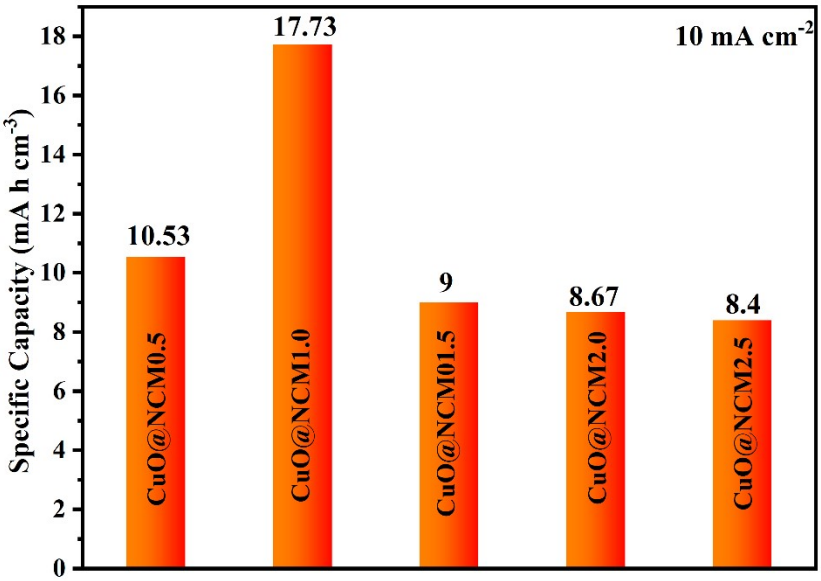

Fig. S5. Volumetric capacity comparison of CuO@NiCoMn-LDH series samples.

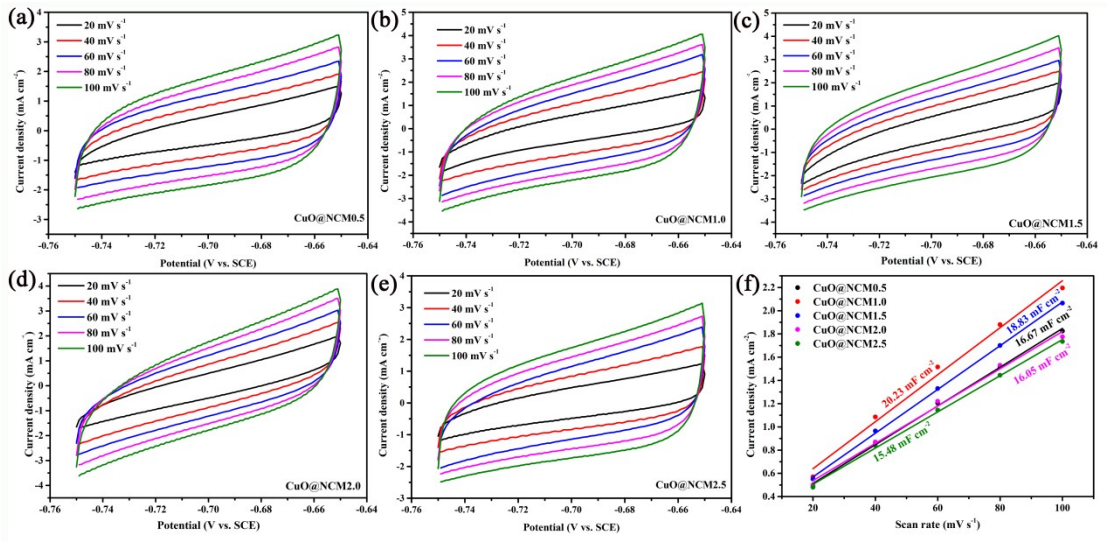

Fig. S6 (a) Cyclic voltammogram curves of CuO@NCM0.5, (b) CuO@NCM1.0, (c) CuO@NCM1.5, (d) CuO@NCM2.0, (e) CuO@NCM2.5 measured in the range of -0.75 ~ -0.65 V at different scan rates: 20, 40, 60, 80, and 100 mV·s^{-1}. (f) Electrochemical double-layer capacitance measurements of samples.

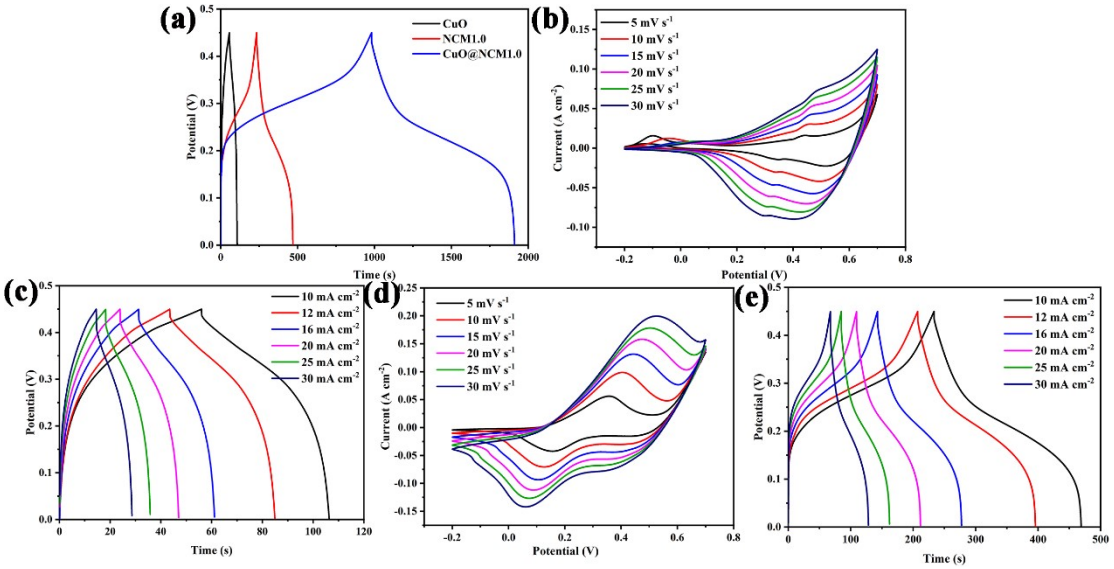

Fig. S7. (a) GCD curves of CuO, NCM1.0 and CuO@NCM1.0 at 10 mA·cm^{-2}. (b-c) CV and GCD curves under different scan rates and different current densities of CuO. (c-d) CV and GCD curves of NCM1.0.

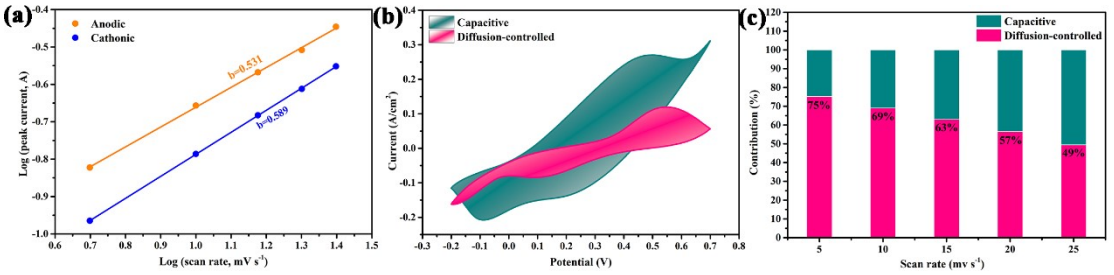

Fig. S8 (a) Logarithmic relationship between anode peak and cathode peak current and scan rate. (b) Capacitive contribution and diffusion contribution of CuO@NiCoMn1.0 electrode at 15 $mV \cdot s^{-1}$. (c) The contribution rate of diffusion control and capacitance control of CuO@NiCoMn1.0 at different scan rates.

Table S1. Performance comparison between CuO@NiCoMn1.0 LDH and other electrode materials.

Electrode material	Electrolyte	Specific capacitance	Cycling stability	Ref.
NiCo@Ni2Co1/CFC	1M KOH	9.67 $F \cdot cm^{-2}$ (at 5 $mA \cdot cm^{-2}$)	75% (2000 cycles at 5 $mA \cdot cm^{-2}$)	[1]
Cu_3N@CoFe-LDH	2M KOH	3.08 $F \cdot cm^{-2}$ (at 1 $mA \cdot cm^{-2}$)	93.9% (10000 cycles at 20 $mA \cdot cm^{-2}$)	[2]
Zn–Ni–Co TOH	1M KOH	2.14 $F \cdot cm^{-2}$ (at 3 $mA \cdot cm^{-2}$)	108.6% (10000 cycles at 100 $mV \cdot s^{-1}$)	[3]
4M-P@NiCo LDH	6M KOH	7 $F \cdot cm^{-2}$ (at 50 $mA \cdot cm^{-2}$)	77.17% (5000 cycles at 10 $A \cdot g^{-1}$)	[4]
H-NiCo LDH@ACC	1M KOH	3.06 $F \cdot cm^{-2}$ (at 1 $mA \cdot cm^{-2}$)	70% (10000 cycles at 80 $mA \cdot cm^{-2}$)	[5]
CCCH@NiCo-LDH NWAs@Au–CuO/Cu fibers	3M KOH	1.97 $F \cdot cm^{-2}$ (at 7.96 $mA \cdot cm^{-2}$)	90.8% (30000 cycles at 7.96 $mA \cdot cm^{-2}$)	[6]
CC/NiCoP@NiCo-LDH	6M KOH	4.683 $F \cdot cm^{-2}$ (at 1 $mA \cdot cm^{-2}$)	81.1% (5000 cycles at 20 $mA \cdot cm^{-2}$)	[7]
CuO@NCM1.0	2M KOH	20.7 $F \cdot cm^{-2}$ (at 10 $mA \cdot cm^{-2}$)	94.82% (3000 cycles at 30 $mA \cdot cm^{-2}$)	This work

Table S2. Comparative areal capacitances, areal energy and power densities of recently reported ASCs with our ASCs.

ASC device	Ca ($F\ cm^{-2}$)	Ea ($mWh\ cm^{-2}$)	Pa ($mW\ cm^{-2}$)	Ref
CoO@MnO_2//AC	0.91	0.37	1.7	[8]
CMO@NS-8//AC	1.16	0.412	4	[9]
$NiCo_2O_4$@CC//ACC	0.75	0.24	0.75	[10]
Co/CoO//AC	1.62	0.51	2.03	[11]
$CuCo_2O_4$/CuO@$NiCo_2S_4$//AC	2.3	0.824	8	[12]
Co_3S_4@Ni_3S_4//PC	0.513	0.19	1.72	[13]
CoAl-LDHs//rGO	1.77	0.71	17.05	[14]
Cu_2S@NiCo-LDH DSNAs//NPC	4.2	1.67	4.25	[15]
CuO@NCM1.0//Fe_3O_4@C/CuO	7.52	2.67	4.79	This work

Reference

1 W. Su, F. Wu, L. Fang, J. Hu, L. Liu, T. Guan, X. Long, H. Luo and M. Zhou, *J. Alloys Compd.*, 2019, **799**, 15-25.

2 X. Zhou, X. Li, D. Chen, D. Zhao and X. Huang, *J. Mater. Chem. A*, 2018, **6**, 24603-24613.

3 Z.-H. Huang, F.-F. Sun, M. Batmunkh, W.-H. Li, H. Li, Y. Sun, Q. Zhao, X. Liu and T.-Y. Ma, *J. Mater. Chem. A*, 2019, **7**, 11826-11835.

4 G. Wang, Z. Jin and W. Zhang, *Dalton Trans*, 2019, **48**, 14853-14863.

5 X. Xuan, M. Qian, L. Han, L. Wan, Y. Li, T. Lu, L. Pan, Y. Niu and S. Gong, *Electrochim. Acta*, 2019, **321**, 134710.

6 Y. Guo, X. Hong, Y. Wang, Q. Li, J. Meng, R. Dai, X. Liu, L. He and L. Mai, *Adv. Funct. Mater.*, 2019, **29**, 1809004.

7 X. Y. Gao, Y. F. Zhao, K. Q. Dai, J. T. Wang, B. Zhang and X. J. Shen, *Chem. Eng. J.*, 2020, **384**, 123373.

8 X. Wang, Y. Xiao, D. Su, L. Zhou, S. Wu, L. Han, S. Fang and S. Cao, *Electrochim. Acta*, 2016, **194**, 377-384.

9 T. Wang, W. Ma, Y. Zhang, J. Guo, T. Li, S. Wang and D. a. Yang, *J. Energy Storage*, 2021, **35**, 102319.

10 H. Zhang, D. Xiao, Q. Li, Y. Ma, S. Yuan, L. Xie, C. Chen and C. Lu, *J. Energy Chem.*, 2018, **27**, 195-202.

11 L. Wang, H. Wang, C. Qing, G. Qu, W. Ma and Y. Tang, *J. Alloys Compd.*, 2017, **726**, 139-147.

12 P. Zhang and H. He, *Appl. Surf. Sci.*, 2019, **497**, 143725.

13 Z. Gao, C. Chen, J. Chang, L. Chen, P. Wang, D. Wu, F. Xu and K. Jiang, *Chem. Eng. J.*, 2018, **343**, 572-582.

14 S. S. Li, P. P. Cheng, J. X. Luo, D. Zhou, W. M. Xu, J. W. Li, R. C. Li and D. S. Yuan, *Nano-Micro Lett.*, 2017, **9**, 31.

15 Z. Yuan, H. Wang, J. Shen, P. Ye, J. Ning, Y. Zhong and Y. Hu, *J. Mater. Chem. A*, 2020, **8**, 22163-22174.